



THE UNIVERSITY *of* EDINBURGH

Edinburgh Research Explorer

Contrast-enhanced CT predictors of lymph nodal metastasis in dogs with oral melanoma

Citation for published version:

Menghini, T, Schwarz, T, Dancer, S, Gray, C, MacGillivray, T & Blacklock, K 2023, 'Contrast-enhanced CT predictors of lymph nodal metastasis in dogs with oral melanoma', *Veterinary Radiology & Ultrasound*, pp. 1-12. <https://doi.org/10.1111/vru.13254>

Digital Object Identifier (DOI):

[10.1111/vru.13254](https://doi.org/10.1111/vru.13254)

Link:

[Link to publication record in Edinburgh Research Explorer](#)

Document Version:

Publisher's PDF, also known as Version of record

Published In:

Veterinary Radiology & Ultrasound

General rights



Copyright for the publications made accessible via the Edinburgh Research Explorer is retained by the author(s) and / or other copyright owners and it is a condition of accessing these publications that users recognise and abide by the legal requirements associated with these rights.

Take down policy

The University of Edinburgh has made every reasonable effort to ensure that Edinburgh Research Explorer content complies with UK legislation. If you believe that the public display of this file breaches copyright please contact openaccess@ed.ac.uk providing details, and we will remove access to the work immediately and investigate your claim.



Contrast-enhanced CT predictors of lymph nodal metastasis in dogs with oral melanoma

Timothy L. Menghini¹  | Tobias Schwarz¹  | Sumari Dancer¹ | Calum Gray² | Tom MacGillivray³ | Kelly L. Bowlt Blacklock¹

¹Hospital for Small Animals, The Royal (Dick) School of Veterinary Studies, The University of Edinburgh, Scotland, UK

²Edinburgh Imaging Facility, Queen's Medical Research Institute, University of Edinburgh, Scotland, UK

³Centre for Clinical Brain Sciences, University of Edinburgh, Scotland, UK

Correspondence

Kelly L. Bowlt Blacklock, Hospital for Small Animals, The Royal (Dick) School of Veterinary Studies, The University of Edinburgh, Scotland, UK.

Email: kelly.blacklock@ed.ac.uk

Present address:

Hospital for Small Animals, The Royal (Dick) School of Veterinary Studies, Easter Bush Campus, Midlothian EH25 9RG, Scotland.

Abstract

Canine oral melanoma (OM) has highly aggressive behavior, with frequent local metastasis. Computed tomography 3D volumetric analysis is an accurate predictor of lymph node (LN) metastasis of oral cancers in humans but whether this is true for dogs with OM is unknown. In this retrospective observational study, CT imaging was used to assess mandibular and retropharyngeal lymphocenter (LC) changes in dogs with nodal metastatic (n = 12) and non-metastatic (n = 10) OM, then these findings were compared with those of healthy control dogs (n = 11). Using commercial software (Analyze, Biomedical Imaging Resource), lymphocenters were defined as regions of interest. LC voxels, area (mm²), volume (mm³), and degree of attenuation (HU) were compared between groups. Mandibular lymphocenter (MLC) metastasis was present in 12 of 22 (54.5%) dogs; no dogs had confirmed retropharyngeal lymphocenter (RLC) metastasis. Mandibular lymphocenter volume was significantly different between positive and negative LCs (median 2221 and 1048 mm³, respectively, $P = 0.008$), and between positive and control LCs (median 880 mm³, $P < 0.01$). There was no evidence of a significant difference in voxel number or attenuation between groups. Mandibular lymphocenter volume moderately discriminated for metastatic status (AUC 0.754 [95% CI = 0.572–0.894, $P = 0.02$]), with a positive predictive value of 57.1% (95% CI = 0.389–0.754). Adjusting for patient weight did not improve discrimination (AUC = 0.659 (95% CI = 0.439–0.879, $P = 0.13$)). In conclusion, these findings suggest 3D CT volume measurement of MLC can predict nodal metastasis in dogs with OM and shows promise but further research, perhaps in combination with other modalities, is required to improve accuracy.

KEYWORDS

canine, mandibular, melanoma, metastasis, node, volume

Abbreviations: LC, lymphocenter; MLC, mandibular lymphocenter; PPV, positive predictive value; RLC, retropharyngeal lymphocenter.

This is an open access article under the terms of the [Creative Commons Attribution-NonCommercial](https://creativecommons.org/licenses/by-nc/4.0/) License, which permits use, distribution and reproduction in any medium, provided the original work is properly cited and is not used for commercial purposes.

© 2023 The Authors. *Veterinary Radiology & Ultrasound* published by Wiley Periodicals LLC on behalf of American College of Veterinary Radiology.

1 | INTRODUCTION

Oral melanoma (OM) is the most common malignant oral tumor in dogs and carries a guarded prognosis due to its highly aggressive behavior.¹ Metastatic disease to regional lymph nodes (LN) is frequent and occurs in 58–80% of canine patients.^{2–4} Nodal metastasis decreases median survival time (MST) in dogs and people with OM.^{5–7} The World Health Organization (WHO) clinical staging system,⁸ used for the determination of extent of neoplastic disease, is of prognostic significance because the metastatic rate of OM is size, stage, and site dependent.⁹ One study found dogs with tumors <2 cm in diameter had a MST of 511 days, versus 164 days for those with tumors >2 cm or with LN involvement.¹⁰ Therefore, accurate staging and early detection of LN metastasis is essential to optimize prognostication and facilitate appropriate patient management.

Detecting LN metastasis is problematic in veterinary clinical practice: LN size or asymmetry on palpation is unreliable for detection of metastasis¹¹; there are significant patient anatomical variation in the number and location of LNs within a lymphocenter (LC)¹²; and complex, variable LN drainage patterns have been described.¹³ Not all LNs are palpable or readily accessible for sampling (e.g., medial retropharyngeal and parotid LCs), which further complicates preoperative decision making.⁴ For this reason, extirpation of all bilateral mandibular and retropharyngeal LCs for histopathology has been recommended to avoid understaging patients,^{14,15} but this is invasive and the therapeutic benefit remains unknown. Sentinel LN (SLN) mapping, such as with indirect CT lymphangiography (CTL), can allow surgeons to remove only potentially clinically relevant LNs by identifying which drain the primary tumor,¹⁶ however a recent study found CTL findings alone cannot diagnose SLN metastasis in dogs with melanoma.¹⁷ Non-invasive techniques to accurately detect LN metastasis will greatly improve management of patients with OM by allowing more selective LN removal. In human medicine, detection of LN metastasis with high diagnostic accuracy has been described using contrast-enhanced computed tomography (CT) texture analysis, and computer-aided 3D measurements of LN volume and attenuation, for a variety of tumors, including oral melanoma.^{7,18,19}

The purpose of this study was to perform 3D LN analysis using CT images from dogs with metastatic and non-metastatic OM to determine if CT findings could predict metastatic status in dogs with OM. We hypothesized that lymphocenters associated with metastatic OM would have significantly higher volume, area, voxel number, and mean attenuation (Hounsfield Units, HU) on CT images compared to dogs with non-metastatic OM. Our secondary hypothesis was there would be good inter- and intraobserver agreement with no significant difference in LC repeated measurements.

2 | MATERIALS AND METHODS

2.1 | Selection and description of subjects

This retrospective, observational study was approved by the University of Edinburgh Veterinary Ethical Review Committee (VERC 09.22.v2).

Medical records from the University of Edinburgh Hospital for Small Animals were searched from 2009 to 2022 for dogs with histopathologically confirmed OM that underwent a head and neck CT with LN sampling performed within 14 days of imaging.

There were three cohorts. The positive group comprised treatment-naïve dogs with nodal metastatic disease (diagnosed via cytology and/or histopathology)²⁰ reported in any mandibular lymphocenter (MLC) or retropharyngeal lymphocenter (RLC).¹⁵ The negative group comprised treatment-naïve dogs with no nodal metastasis (diagnosed via histopathology) in any extirpated MLC or RLC. The control group comprised adult dogs that underwent CT scan between 2009 and 2022 for diagnosis of cervical intervertebral disc disease but were otherwise healthy with no concurrent neoplasia, lymphadenopathy, or inflammatory disease (e.g., otitis). Final decisions over subject inclusion/exclusion were made by a European College of Veterinary Surgeons-certified surgeon (K.B.B.) and an American College of Veterinary Radiology/European College of Veterinary Diagnostic and Imaging-certified veterinary radiologist (T.S.). All histopathological or cytological analyses were conducted by a European College of Veterinary Pathologists-certified pathologist at the same institution. Sentinel LN mapping was not performed for any patient in this study. Clinical patient data collected included: signalment, age, weight, and histopathologic diagnosis. Recording of clinical data was performed by an American College of Veterinary Surgeons resident (T.L.M.) under supervision of a European College of Veterinary Surgeons-certified surgeon (K.B.B.).

2.2 | Data recording and analysis

Images were assessed using open-source software (Horos, Horos Project, Geneva, Switzerland) and DICOM files imported into an image analysis workstation (Analyze 12.0, Biomedical Imaging Resource, Mayo Clinic, Rochester, Minnesota, USA) for evaluation.

Lymphocenter-specific regions of interest (ROI) were created by a single observer (T.L.M.) tracing the perimeter of each mandibular lymph node (MLN) and retropharyngeal lymph node (RLN) on post-contrast CT transverse slices. Regions of interest were verified by an American College of Veterinary Radiology/European College of Veterinary Diagnostic and Imaging-certified radiologist (T.S.) who was blinded to patient metastatic status. Perinodal fat or air was excluded where present by visual assessment.

Dogs have two to three MLNs per side, occasionally up to 5,¹⁵ so all MLNs visible on CT were labeled. The RLC consists of a medial RLN (MRLN), and sometimes a lateral RLN (30% dogs).¹⁵ Every LN within each ipsilateral LC was outlined in the same color and grouped for analysis, resulting in four ROI/lymphocenters: left MLC, right MLC, left RLC, and right RLC (Figure 1). In the positive and negative groups, only LCs with known histopathology or cytology were labeled. This assumed the entire ROI had the same metastatic status. Histopathologically negative LCs were not included from positive dogs with metastatic disease in other LCs. In the control group, all four LCs were labeled. All ROIs were then propagated between labeled slices to generate a 3D rendering (Figure 1C,F). Each ROI was sampled individually

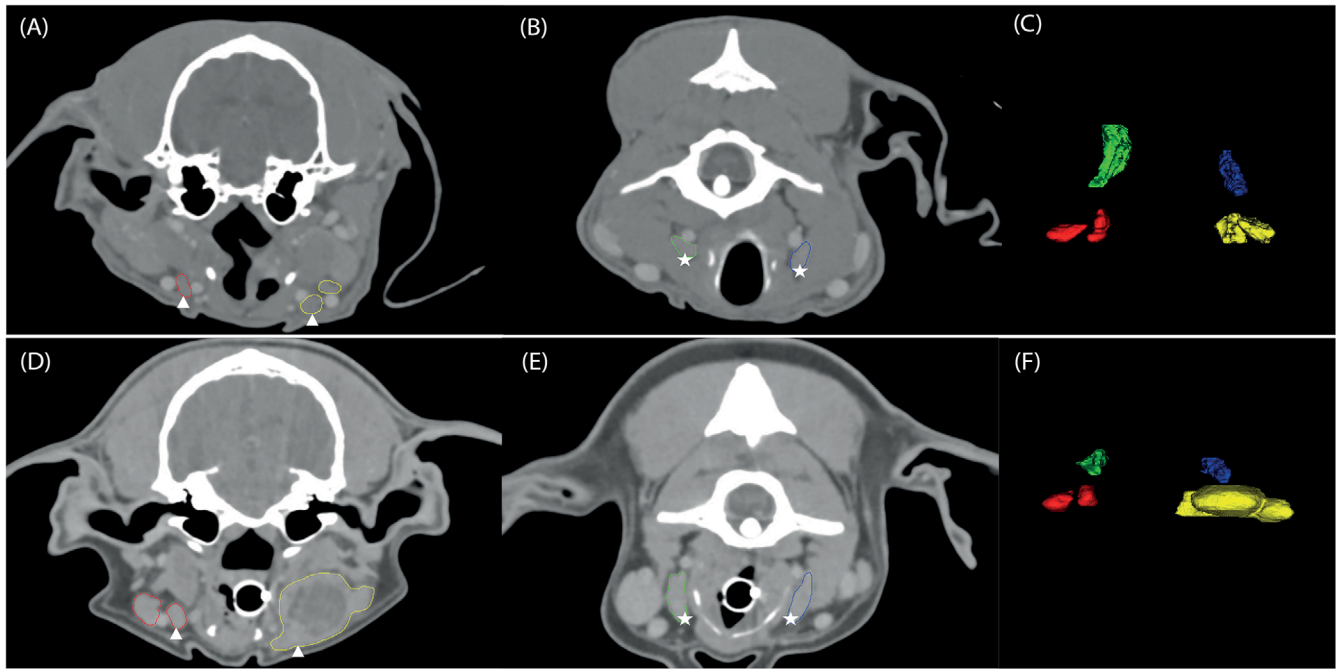


FIGURE 1 Transverse contrast-enhanced head CT images and 3D volume renderings of mandibular lymphocenters (MLC) and retropharyngeal lymphocenters (RLC) [soft tissue algorithm, 120 kVp, 200 mAs, 1.0 s/rotation, 1.0 mm slice thickness, window width = 350, window level = 60]. Patient's right is in left of image. Top, Normal MLC (A), RLC (B), and 3D volume rendering of all four lymphocenters (C, front view) in a control dog. Bottom, enlarged metastatic right MLC (D), negative RLC (E) and 3D volume rendering of all 4 lymphocenters (F, front view) in a positive dog (Case #6). Note the extremely large right MLC compared to others, indicating macrometastasis. Circled areas indicate regions of interest (ROI). Red = right MLC(s); yellow = left MLC(s); green = right RLC and blue = left RLC. White arrowheads indicate MLCs; White stars indicate RLCs. [Color figure can be viewed at wileyonlinelibrary.com]

without combining or summing objects and all slices were sampled. Data generated for each ROI included: maximum, minimum, and mean attenuation in Hounsfield units (\overline{HU}), standard deviation (SD), number of voxels, area (mm^2), and volume (mm^3). Regions of interest data were calculated automatically using the Analyze software system and volume rendering algorithms.²¹ \overline{HU} is the average of all voxel postcontrast attenuation measurements. A voxel is simply the 3D equivalent to a pixel, whereby its size is related to pixel size and slice thickness. Pixel size is equal to the field of view (FOV) divided by the matrix size. As slices were acquired contiguously, voxel depth was equal to slice thickness. As each ROI is made up of numerous cuboid shaped voxels, the software computes the ROI measurements using discrete mathematical formulae where: Area = total voxel length (mm) \times width (mm); and Volume = area (mm^2) \times voxel depth (mm). This means for non-uniform shapes such as tumors or LNs, volume can be measured by quantifying the number of voxels within a 3D ROI. For example, in a scan with 512×512 matrix size, 200 mm FOV, and 0.7 mm slice thickness, each voxel represents a volume of $\sim 0.106812 \text{ mm}^3$.

For additional detail pertaining to LN labeling and voxel sizes, see Supporting Information.

Region of interest measurements were repeated 10 times by the initial observer (T.L.M.) and a blinded European College of Veterinary Diagnostic and Imaging-certified veterinary radiologist (S.D.) for intraobserver and interobserver agreement. Ten CT scans were selected to review using a random number generator (<https://www.random.org>)

in a blinded independent session, using the described method.

2.3 | Statistics

Statistical analyses were performed using commercially available software (SPSS, v24.0; and R, v4.1.0) by a veterinary surgeon with a PhD (K.B.B.) and a resident with post-graduate course level training in statistics (T.L.M.), after consultation from a statistician during the study design. Voxels, area, and volume values were \log_{10} -transformed and values for each ROI standardized to the control population. \log_{10} -transformation was not possible for negative \overline{HU} values (range -26.089 to 123.02), therefore these values were standardized to the control population for both pre- and postcontrast datasets. The transformed and standardized data were analyzed using a linear mixed-effects model (lme4 package) with Tukey HSD post hoc test to identify correlation between voxel, area, volume, or \overline{HU} with LC metastatic or non-metastatic status. Graphical data representation was performed using ggplot. For significant variables, a ROC curve was generated to identify sensitivity/specificity and positive/negative predictive values (PPV/PNV) for prediction of metastatic status.

Bland-Altman (BA) plots²² and a one-sample *t*-test were used to assess intra- and inter-observer agreement for ROI measurements. For intraobserver testing, values for volume, area, and voxel number were

TABLE 1 Number of lymphocenters (and total lymph nodes) analyzed by group and location for all dogs (n = 33).

	Right MLC	Left MLC	Right RLC	Left RLC	Total
Dogs with metastatic disease (n = 12)	7 (14)	7 (13)	0	0	14 (27)
Dogs with non-metastatic disease (n = 10)	9 (21)	9 (25)	4 (4)	5 (5)	27 (55)
Control dogs (n = 11)	9 (19)	8 (20)	11 (11)	11 (11)	39 (61)
Total					80 (143)

MLC = mandibular lymphocenter node; RLC = retropharyngeal lymphocenter.

\log_e -transformed prior to statistical analysis. For all analyses, $P < 0.05$ was considered significant.

3 | RESULTS

3.1 | Study population

Twelve dogs were enrolled in the positive group, 10 in the negative group, and 11 in the control group (33 dogs total). Breeds were Labrador Retriever (n = 6), mixed breed (n = 6), Golden Retriever (n = 5), Cocker Spaniel (n = 4), and one each of 13 other breeds (Table S1). At time of CT, mean patient age (in years) was 10.7 (± 2.0) in the positive group, 10.5 (± 2.0) in the negative group, and 6.6 (± 3.4) in controls. Mean bodyweight was 27.2 kg (± 10.9) in the positive group, 23.3 kg (± 11.9) in the negative group, and 19.3 kg (± 10) in controls. Sex distribution was male (5), female (4), neutered male (16), and neutered female (8).

3.2 | Lymph node inclusion

One hundred forty-three LNs from 33 dogs were analyzed on CT (Table 1). This comprised 112 MLNs and 31 MRLNs. Median time between CT and LN sampling was 3.5 days (range 0–14). Twelve of 22 dogs with OM (54.5%) were positive for nodal metastasis.

In the positive group, 14 LCs (comprising 27 nodes) were analyzed. All 14 LCs associated with metastatic disease were MLCs (7 right, 7 left). Of the 12 positive dogs, 10 had histologic nodal macrometastasis and two had micrometastasis.²⁰ Ten dogs had unilateral MLC metastatic spread, ipsilateral to the primary OM, and two had bilateral metastasis. Eleven positive dogs had two MLNs per side; one had an extremely large left MLN that encompassed all MLNs on that side (Figure 1D). There were no RLCs in the positive group as no MRLNs in any dog had demonstrable histologic or cytologic metastasis during the study period.

In the negative group, 27 LCs (comprising 55 LNs) were analyzed from 10 dogs. All LNs included in this group were histologically negative for metastasis.

Thirty-nine LCs (comprising 61 LNs) were analyzed from 11 dogs in the control group. Five MLCs were excluded from three control dogs because the entire LC was not scanned on CT. Median number of MLNs

measured per side on CT was 2 for all groups (range 1–4). There were no lateral RLNs in any dog.

3.3 | CT lymphocenter analysis

Eighteen of 33 dogs had 64-slice CT performed (after 2016); 15 of 33 dogs had 4-slice CT performed (prior to 2016). Window width and level were manually altered to optimally visualize LNs and were all between –428 and 514 HU. Further details of CT imaging acquisition are available in Table S2. Measurements of volume, area, and voxel number were identical between pre- and postcontrast CT for all groups (Table S3). Only \overline{HU} values differed between pre- and postcontrast images. Summary of ROI measurements of volume, area, voxels, and \overline{HU} are listed in Table 2.

The results of the linear mixed-effects models are illustrated in Figure 2 for standardized voxels, area, volume, and \overline{HU} .

The P -values generated for the linear mixed-effects model with Tukey HSD post hoc test are shown in Table 3. LC volume was larger in positive than negative LCs (median 2221 mm³ [range 333–14892 mm³] and 880 mm³ [range 185–2175 mm³], respectively, $P = 0.004$), and in positive versus control LCs (median 2221 mm³ [range 333–14892 mm³] and 886 mm³ [range 290–2048 mm³], respectively, $P = 0.002$).

The difference in area between positive and negative LCs was statistically significant ($P = 0.017$) but was not different between positive and controls ($P = 0.077$), or negative and controls ($P = 0.806$).

The statistical analysis was repeated following exclusion of RLC values for the negative and control group, because no MRLNs were included in the positive cohort. The results of the linear mixed-effects models are illustrated in Figure 3 for standardized voxels, area, volume and \overline{HU} of MLCs only.

The P -values generated for the linear mixed-effects model with Tukey HSD post hoc test performed on only MLCs are shown in Table 4. MLC volume was statistically different between positive and negative LCs (median 2221 mm³ [range 333–14 892 mm³] and 1048 mm³ [range 403–2175 mm³], respectively, $P = 0.008$), and between positive and control LCs (median 2221 mm³ [range 333–14 892 mm³] and 880 mm³ [range 349–1371 mm³], respectively, $P < 0.01$). The difference in area of the MLCs between positive and negative LCs was again statistically significant ($P = 0.033$) but not between positive and controls.

TABLE 2 Summary ROI measurements of volume (mm^3), area (mm^2), voxel number and degree of attenuation (mean HU) between groups. Data reported as mean \pm standard deviation.

Group	Volume (mm^3)	Area (mm^2)	Voxels	Mean attenuation post contrast (HU)
Positive	4084 \pm 4361	4439 \pm 5990	29 316 \pm 49 305	71 \pm 13
Negative	997 \pm 528	1219 \pm 713	9650 \pm 5870	66 \pm 17
Controls	960 \pm 443	1215 \pm 643	14 991 \pm 10 443	67 \pm 27.64

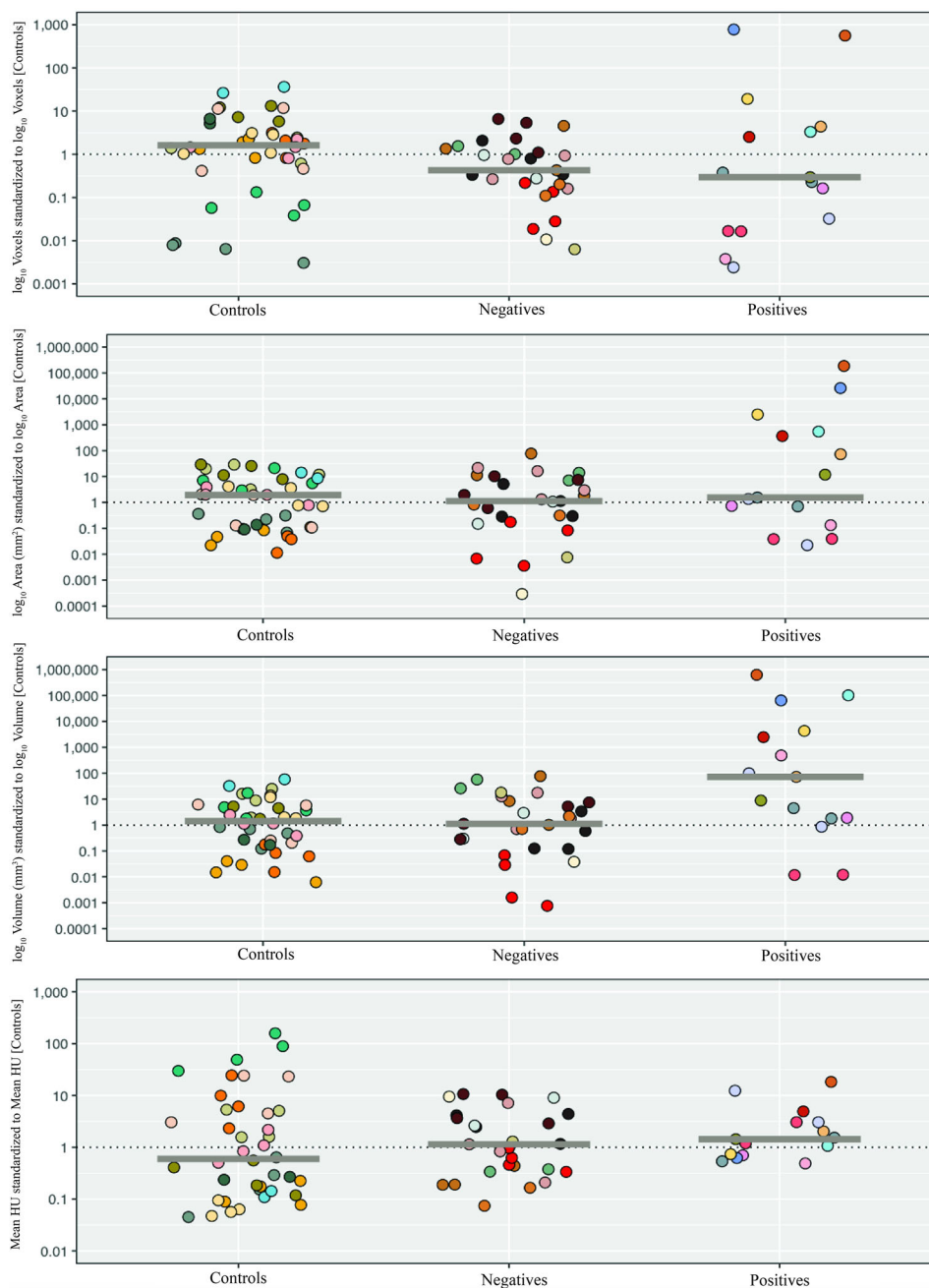


FIGURE 2 Comparison of standardized measurements of mandibular and retropharyngeal lymphocenters from dogs with oral melanoma (metastatic [positives] and non-metastatic [negatives]) and with no neoplastic disease [controls]. Individual dots represent ROI. [Color figure can be viewed at wileyonlinelibrary.com]

TABLE 3 Results of p-values generated for the linear mixed-effects model with Tukey HSD post-hoc test of lymphocenters from dogs with metastatic (positive) or non-metastatic (negative) oral melanoma, and dogs with no neoplastic disease (control).

	P-value		
	Negative-control	Positive-control	Positive-negative
Voxels*	0.400	0.986	0.483
Area*	0.806	0.077	0.017
Volume*	0.999	0.002	0.004
\overline{HU} **	0.949	0.862	0.709

*Log10 and standardized values.

**Standardized values (Mean attenuation in Hounsfield units).

TABLE 4 Results of p-values generated for the linear mixed-effects model with Tukey HSD post-hoc test of only mandibular lymphocenters from dogs with metastatic (positive) or non-metastatic (negative) oral melanoma, and dogs with no neoplastic disease (control).

	p-value		
	Negative-control	Positive-control	Positive-negative
Voxels*	0.887	0.868	0.565
Area*	0.981	0.065	0.033
Volume*	0.789	<0.01	0.008
\overline{HU} **	1.000	0.609	0.602

*Log10 and standardized values.

**Standardized values (Mean attenuation in Hounsfield units).

There was no significant difference in number of voxels or \overline{HU} between positive and negative LCs or versus controls (Table 2), even after excluding RLCs (Table 4).

Receiver operating characteristic (ROC) curves generated are shown in Figure 4. The area under the curve (AUC) generated using MLC volume as a predictor of metastatic status was 0.754 (95% confidence interval, CI = 0.572–0.894, $P = 0.02$), which was statistically significant but offers only moderate discrimination. Attempting to adjust for MLC volume using patient weight (volume [mm³]/weight [kg]) did not improve discrimination (AUC = 0.659, CI = 0.439–0.879, $P = 0.13$) (Figure 4). Using a cut off of 1371 mm³ (the largest measured control MLC volume), sensitivity and specificity of volume as a predictor of metastatic disease were 64.3% and 72.2%, respectively; with a PPV of 57.1% (CI = 0.389–0.754) and NPV of 68.4% (CI = 0.502–0.866).

3.4 | Intraobserver and interobserver agreement

Ten randomly selected ROIs were re-measured from four positive, three negative, and three control dogs. Results of intraobserver and interobserver agreement are shown in Table 5. All repeated measurements showed no significant difference in LC \overline{HU} , voxels, area, and volume between the first and second measurements (Table 5).

When assessing intraobserver accuracy, there was no significant difference in LC volume, area or voxel number (Figure 5A–C) after log_e

transformation (mean difference -0.06 ± 0.11 SD, $P = 0.10$), or \overline{HU} without transformation (Figure 5D; mean difference 1.97 ± 4.94 HU SD, $P = 0.24$).

Between observers, there was no significant difference in LC volume (Figure 6A; mean difference -4.96 mm³ \pm 160.24 mm³ SD, $P = 0.93$), area (Figure 6B; (mean difference 1.24 mm² \pm 217.98 mm² SD, $P = 0.99$), voxel number (Figure 6C; mean difference 22.5 ± 1217.64 SD, $P = 0.96$), or \overline{HU} (Figure 6D; mean difference 1.54 HU \pm 217.98 HU SD, $P = 0.99$).

4 | DISCUSSION

The main finding of this study was that there was a significant difference in 3D propagated CT measurements of LC volume between metastatic and non-metastatic MLCs in dogs with OM, and between metastatic LCs and LCs from a control population. Therefore, we could partially accept our primary hypothesis that LCs from dogs with metastatic OM would have significantly higher volume on CT images compared to dogs with non-metastatic OM. We found histologically negative LCs did not significantly differ in volume, area, voxel number or level of attenuation compared to control LCs.

Mandibular lymph node size on palpation is unreliable for prediction of metastasis (70% sensitivity, 51% specificity),¹¹ because lymphadenomegaly can occur for non-neoplastic reasons such as inflammation.

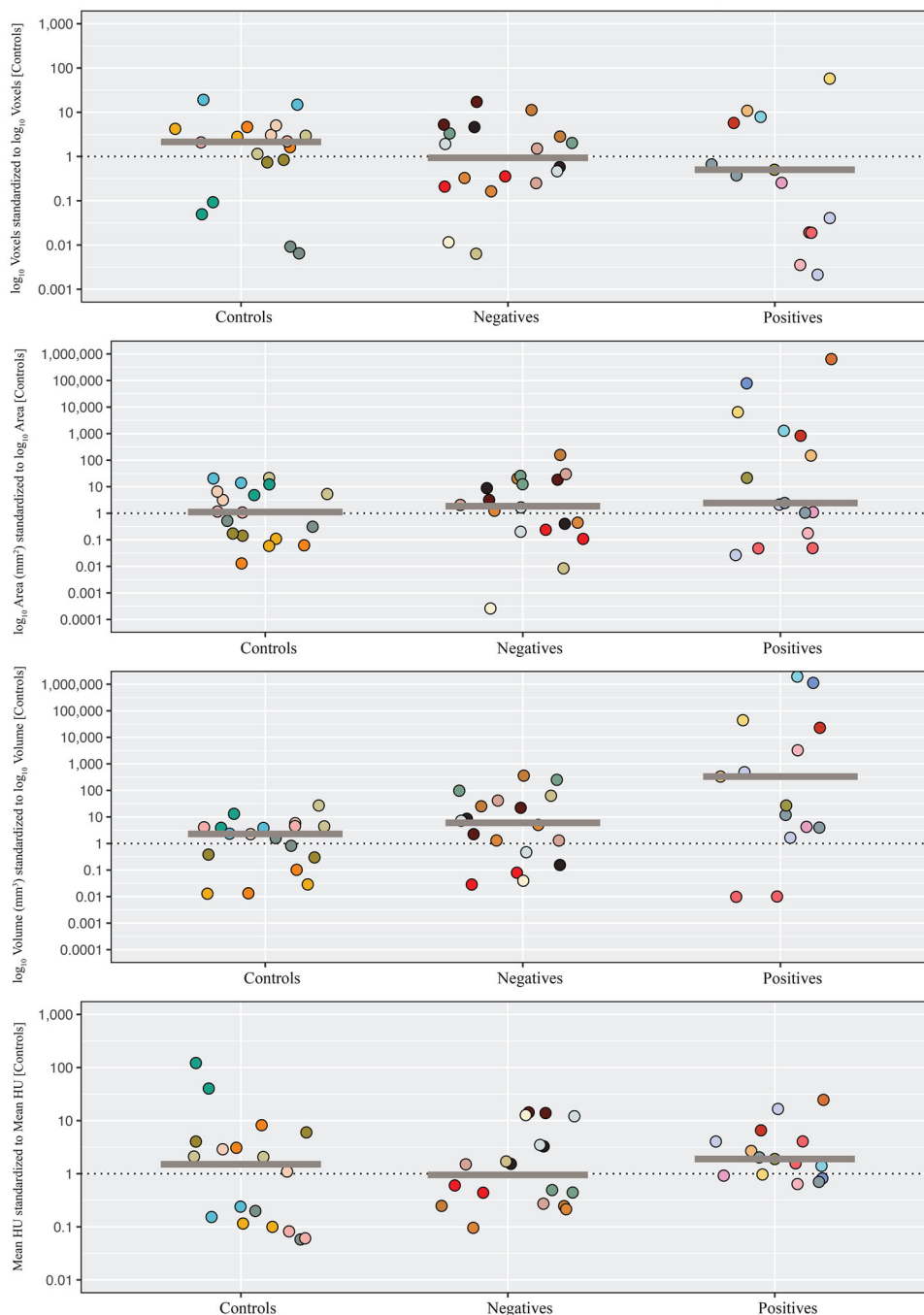


FIGURE 3 Comparison of standardized measurements of only the mandibular lymphocenters (MLCs) from dogs with oral melanoma (metastatic [positives] and non-metastatic [negatives]) and with no neoplastic disease [controls]. [Color figure can be viewed at wileyonlinelibrary.com]

TABLE 5 Intraobserver and interobserver agreement for volume, area, voxel, and mean attenuation (HU) measurements ($n = 10$ lymphocenters).

Measurement	Intraobserver mean difference (\pm SD)	P value	Interobserver mean difference (\pm SD)	P value
Volume (mm^3)	-0.06 (\pm 0.11)	0.10	-4.96 (\pm 160.24)	0.93
Area (mm^2)	-0.06 (\pm 0.11)	0.10	1.24 (\pm 217.98)	0.99
Voxels	-0.06 (\pm 0.11)	0.10	22.5 (\pm 1217.64)	0.96
$\overline{\text{HU}}$	1.97 (\pm 4.94)	0.24	1.54 (\pm 217.98)	0.99

SD, standard deviation. $P < 0.05$ was significant.

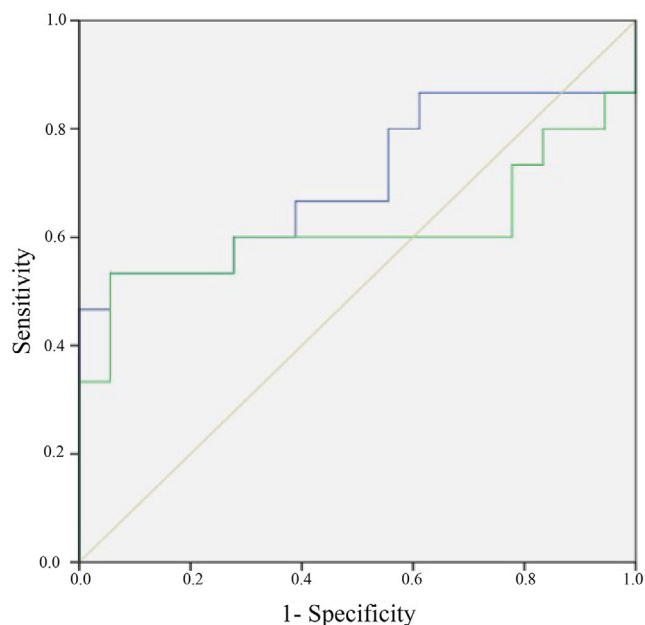


FIGURE 4 Receiver operating characteristic (ROC) curve for prediction of MLC metastasis based on volume (mm^3) [blue], and volume (mm^3) divided by patient weight (kg) [green]. Reference line is shown in yellow. [Color figure can be viewed at wileyonlinelibrary.com]

Approximately 30% of OM metastatic positive dogs have palpably normal sized LNs whereas 70% have enlarged LNs.¹¹

According to Response Evaluation Criteria for Solid Tumors (RECIST),²³ LN measurement is key for categorization of patients into complete versus partial response or stable versus progressive disease, yet contemporary guidelines rely on CT transverse long and short axis 2D measurements.

Computed tomography is an ideal modality for measuring LNs due to its outstanding spatial resolution.²³ However, inconsistency in methodology regarding LN measurement is commonplace in veterinary studies,^{13,24} which limits translation of research findings into clinical use. We are unaware of any studies describing computer-assisted 3D LN measurements in dogs with melanoma. Whole lesion analysis of tumors and LNs has been shown in humans to be more representative of heterogeneity than cross-sectional area.²⁵

A recent canine CT study measured MLN and MRLN size (by short axis width and long-short axis ratio), attenuation, and enhancement pattern, but no CT characteristic was predictive of nodal metastasis.²⁴ Our findings partly support these as we also found no significant difference in attenuation between groups. The lower \overline{HU} levels we found could be due to institutional protocols, regional differences in phenotype, or there being only 11 dogs with OM in that study.²⁴ Interestingly, studies of canine mammary tumors have found differences in attenuation between positive and negative inguinal LNs.²⁶

A previous study approximated sternal LN volume by using length, width, and height measurements on 2D CT images in healthy dogs,²⁷ but this can be affected by measurement on non-acquisition planes and possible oblique LN orientation.²⁸ Three-dimensional volume measurements may be more accurate, but further research is required to

assess this hypothesis in veterinary patients. A study of 3D LN measurements in human patients with lung cancer found nodal volume of $>1282 \text{ mm}^3$ was 76% accurate for diagnosing metastasis.¹⁹ The same study found CT values of $>102 \text{ HU}$ were highly specific (97%), but low sensitivity (18%) meant it was too poor for clinical use. Our results are similar as although we found a significant association between MLC volume and metastasis, it was not strong enough to be clinically useful based on ROC analysis ($\text{AUC} = 0.754$). Area under the curve values of 0.8–0.9 are considered excellent; >0.9 is outstanding.²⁹

Median 3D CT volume measurements of normal canine MLNs and MRLNs using a similar method have been reported to be 260 and 540 mm^3 , respectively,²⁸ but importantly this study only measured a single MLN in each case whereas we included the entire LC. We showed the ability of 3D volumetric CT measurements to detect true metastatic positive or negative MLCs was low (PPV 57.1%, NPV 68.4%), meaning approximately 36% of all MLCs with a volume $> 1371 \text{ mm}^3$ may not be metastatic (64.3% sensitivity and 72.2% specificity).

Nodal metastasis was present in 12 of 22 (54.5%) of dogs with OM in this study, which is similar to other studies.¹¹ All positive dogs in our study had MLC metastasis. One dog also had ipsilateral tonsillar metastasis, although tonsils were not included in our ROI measurements. Ten of 12 (83%) dogs had ipsilateral metastasis whereas two dogs (17%) had bilateral, which is a lower rate of contralateral dissemination than has been reported previously (up to 62%).¹³ No dogs in our study had MRLN metastasis, which meant we were unable to predict RLC metastasis. Only seven of 22 dogs with OM underwent bilateral MLC and RLC extirpation and five dogs had a single MLC removed. One study suggested evaluation of a single MLN is insufficient to definitively rule out LN metastasis in dogs with OM.¹⁵ MLNs are often the first LC that tumors of the head will metastasize to, although some dogs develop “skip” metastases in other LCs without apparent MLN metastases.^{4,30} It is possible that dogs with metastatic RLCs may have been underrepresented and not evaluated on CT or had undetected metastatic LNs if they were not surgically removed. Bilateral RLC and MLC removal with histopathology is now routinely offered at our institution for oral neoplasms,¹⁴ although SLN mapping is gold standard.¹⁶

We showed good intraobserver and interobserver agreement between measurements. Therefore, we could accept our secondary hypothesis of no significant difference in repeated measurements, and that our ROI measurement is reliable and repeatable in this population. We used the BA method because intraclass correlation coefficients (ICC) only assess the strength of a relationship, not agreement.²² Therefore, data with poor agreement can have high correlation. Nevertheless, excellent intraobserver and interobserver correlation ($\text{ICC} > 0.9$) for MLN and MRLN measurements on transverse CT images has been reported in dogs with histologically confirmed OM.³¹ This indicates measurements by different observers has minimal impact on clinical decision making and supports our findings.

This pilot study did have limitations owing to its retrospective nature. It is possible that the low number of dogs and positive LNs may have been underpowered due to sample size. Computed tomography protocol varied regarding slice thickness, voxel size, and CT machines.

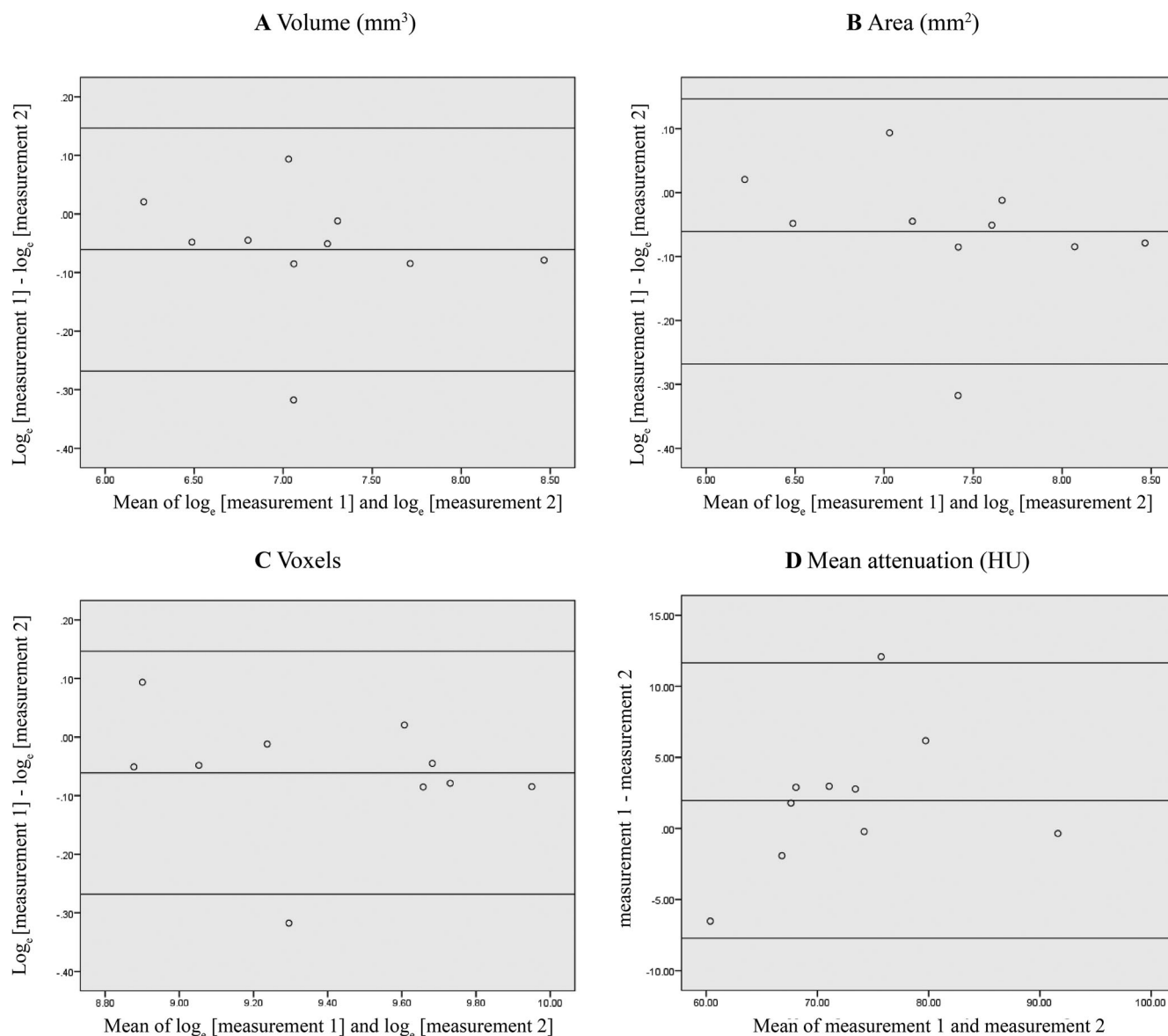


FIGURE 5 Bland–Altman plots of intraobserver agreement between two paired measurements by the initial reviewer (measurement 1 and measurement 2) versus the mean of the two measurements from 10 random dogs. Lines represent mean difference and 95% CI.

Smaller slice thickness of 0.5 or 1 mm for all dogs would reduce partial volume averaging, especially significant in smaller patients. Protocol differences were minor but could explain why we found no significant differences in LC voxel number, level of attenuation, or area between positive and negative dogs. Standardized timing following intravenous contrast administration should be considered in future studies for LC measurement. Small voxel PET-CT shows promise in humans with oral cancer, with reports of increased sensitivity over MRI or CT alone,³² but this has not been shown in dogs to date.²⁶ Prospective case recruitment would allow uniformity of image acquisition.

We chose to consider all MLNs in the ipsilateral LC as a single ROI, but excluded LCs without histopathology/cytology results. This was necessary because our surgeons routinely extirpate all MLNs in cases with multiple ipsilateral MLNs and the number of MLNs per side was

not always listed in surgery or histopathology reports. This may have influenced our results and may not be true of other institutions. It is possible that small changes of individual LNs in dogs with multiple MLNs may not be detected using the method described in this study.

In control dogs, we included all MLNs visible on CT in the ROI. This may have reduced the difference compared to other groups as more LNs could have been included. Control dogs were all adult dogs of similar size with no lymphadenopathy or neoplasia. We chose adult dogs because studies have shown juvenile dogs can have larger LNs.³³ We also did not have ethical approval for prospective CTs of normal dogs.

We included four positive dogs diagnosed by cytology because preoperative cytologic evaluation of MLNs concurs with histologic analysis in >90% of cases.⁴ Nevertheless, cytology may not correlate with histology.²⁰ Therefore, dogs with cytologically diagnosed

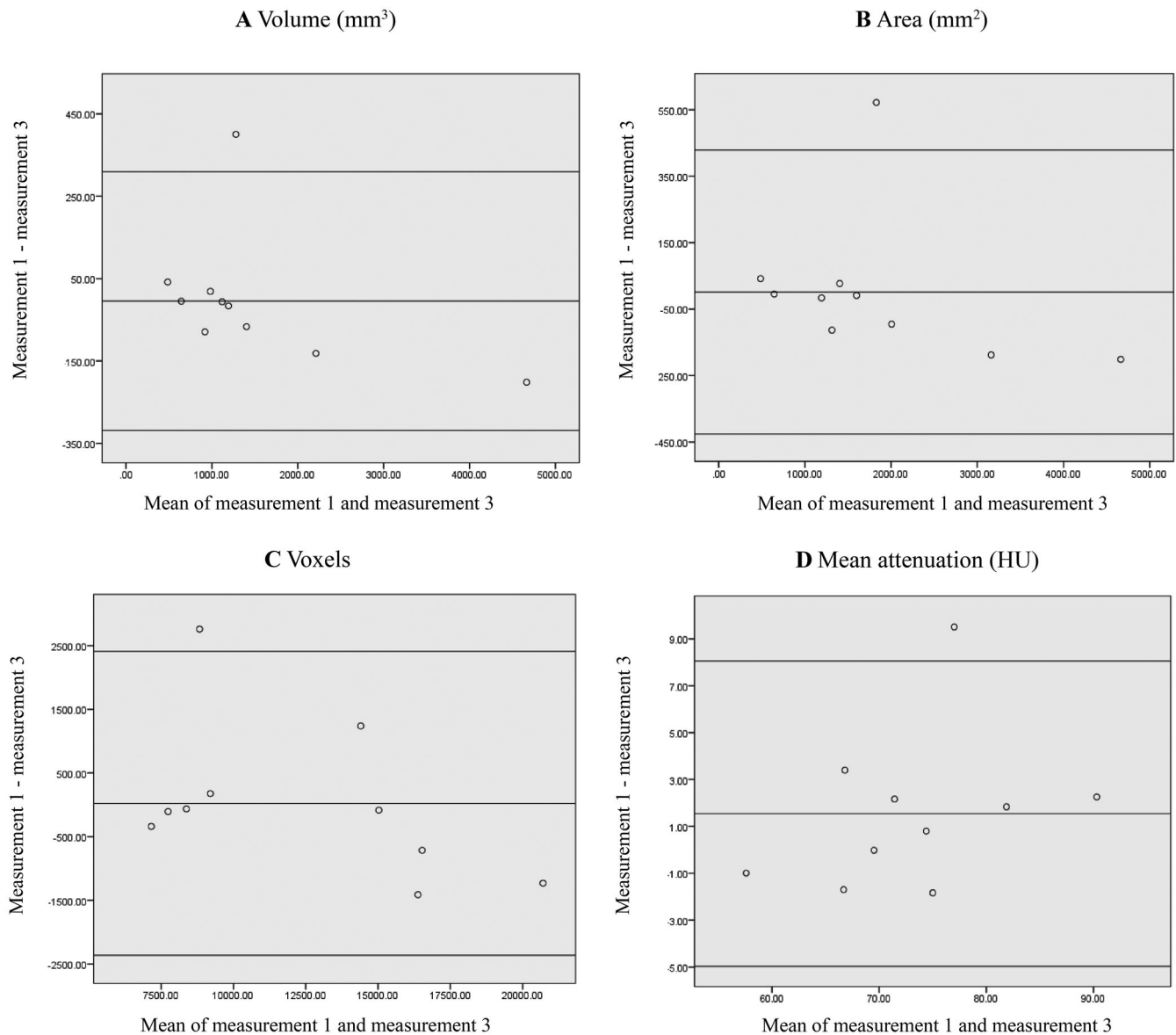


FIGURE 6 Bland–Altman plots of interobserver agreement between the first measurement by the initial reviewer (measurement 1) and measurement by a second reviewer (measurement 3) versus the mean of the two measurements from 10 random dogs. Lines represent mean difference and 95% CI.

metastasis may have been negative had histopathology been performed.³⁴ We routinely offer immunohistochemistry (using PNL-2 or Melan-A markers)³⁵ in equivocal cases, but was not always historically pursued.

Future studies could investigate LN shape or texture CT parameters such as entropy, skewness, and kurtosis in dogs with OM. We believe 3D CT LN analysis has huge potential to improve treatment decision making in veterinary medicine but requires further study to improve accuracy. If protocols are developed to predict nodal metastasis, this information could better inform surgeons.

5 | CONCLUSION

The current study demonstrates that MLC volume is significantly greater on contrast-enhanced CT in dogs with metastatic OM compared to dogs with OM without nodal metastasis, or unaffected control dogs. However, due to only moderate discrimination we cannot yet recommend this modality in the clinical setting to accurately determine metastatic status. Further studies are warranted to improve CT accuracy for prediction of LN metastasis, or of other parameters in relation to metastatic status.

AUTHOR CONTRIBUTIONS

Category 1

- (a) Conception and Design: Menghini, Bowlt-Blacklock
- (b) Acquisition of Data: Menghini, Schwarz, Dancer, Gray, MacGillivray, Bowlt-Blacklock
- (c) Analysis and Interpretation of Data: Menghini, Bowlt-Blacklock

Category 2

- (a) Drafting article: Menghini
- (b) Revising Article for Intellectual Content: Menghini, Schwarz, Dancer, Gray, MacGillivray, Bowlt-Blacklock

Category 3

- (a) Final Approval of the Completed Article: Menghini, Schwarz, Dancer, Gray, MacGillivray, Bowlt-Blacklock

Category 4

- (a) Agreement to be accountable for all aspects of the work in ensuring that questions related to the accuracy or integrity of any part of the work are appropriately investigated and resolved: Menghini, Schwarz, Dancer, Gray, MacGillivray, Bowlt-Blacklock

ACKNOWLEDGMENTS

The authors are grateful to Darren Shaw BSc, PhD, FRSB for statistical advice, and to the caregivers who gave permission to include their pets in this study following diagnosis.

CONFLICT OF INTEREST STATEMENT

The authors declare no conflict of interest.

REPORTING GUIDELINE DISCLOSURE

No STROBE or other reporting guideline checklist was used.

PREVIOUS PRESENTATION OR PUBLICATION

DISCLOSURE

The findings of this study have not been presented at a scientific meeting or published in abstract form.

ORCID

Timothy L. Menghini  <https://orcid.org/0000-0002-4079-3207>

Tobias Schwarz  <https://orcid.org/0000-0001-8412-573X>

REFERENCES

1. Todoroff R, Brodey R. Oral and pharyngeal neoplasia in the dog: a retrospective survey of 361 cases. *J Am Vet Med Assoc.* 1979;175(6):567-571.
2. Tuohy JL, Selmic LE, Worley DR, Ehrhart NP, Withrow SJ. Outcome following curative-intent surgery for oral melanoma in dogs: 70 cases (1998–2011). *J Am Vet Med Assoc.* 2014;245(11):1266-1273. doi:10.2460/javma.245.11.1266
3. Harvey HJ, MacEwen EG, Braun D, Patnaik AK, Withrow SJ, Jongeward S. Prognostic criteria for dogs with oral melanoma. *J Am Vet Med Assoc.* 1981;6(178):580-582.
4. Herring ES, Smith MM, Robertson JL. Lymph node staging of oral and maxillofacial neoplasms in 31 dogs and cats. *J Vet Dent.* 2002;19(3):122-126. doi:10.1177/089875640201900301
5. Kudnig ST, Ehrhart N, Withrow SJ. Survival analysis of oral melanoma in dogs. *Vet Cancer Soc Proc.* 2003;23:39.
6. Overley B, Goldschmidt M, Shofer F. Canine oral melanoma: a retrospective study. *Vet Cancer Soc Proc.* 2001; 21:43. doi:10.3390/vetsci3010007
7. Smith AD, Gray MR, delCampo SM, et al. Predicting overall survival in patients with metastatic melanoma on antiangiogenic therapy and RECIST stable disease on initial posttherapy images using CT texture analysis. *Am J Roentgenol.* 2015;205(3):W283-W293. doi:10.2214/ajr.15.14315
8. Owen L. *TNM classification of tumors in domestic animals.* World Health Organization 1980;
9. Hahn KA, DeNicola DB, Richardson RC, Hahn EA. Canine oral malignant melanoma: prognostic utility of an alternative staging system. *J Small Anim Pract.* 1994;35(5):251-256. doi:10.1111/j.1748-5827.1994.tb03273.x
10. MacEwen EG, Patnaik AK, Harvey HJ, Matus AAH, Matus R. Canine oral melanoma: comparison of surgery versus surgery plus corynebacterium parvum. *Cancer Invest.* 1986;4(5):397-402. doi:10.3109/07357908609017520
11. Williams LE, Packer RA. Association between lymph node size and metastasis in dogs with oral malignant melanoma: 100 cases (1987-2001). *J Am Vet Med Assoc.* 2003;222(9):1234-1236. doi:10.2460/javma.2003.222.1234
12. Langenbach A, McManus PM, Hendrick MJ, Shofer FS, Sorenmo KU. Sensitivity and specificity of methods of assessing the regional lymph nodes for evidence of metastasis in dogs and cats with solid tumors. *J Am Vet Med Assoc.* 2001;218(9):1424-1428. doi:10.2460/javma.2001.218.1424
13. Skinner OT, Boston SE, Souza CH, de M. Patterns of lymph node metastasis identified following bilateral mandibular and medial retropharyngeal lymphadenectomy in 31 dogs with malignancies of the head. *Vet Comp Oncol.* 2017;15(3):881-889. doi:10.1111/vco.12229
14. Green K, Boston SE. Bilateral removal of the mandibular and medial retropharyngeal lymph nodes through a single ventral midline incision for staging of head and neck cancers in dogs: a description of surgical technique. *Veterinary and Comparative Oncology.* 2015;15(1):208-214. doi:10.1111/vco.12154
15. Grimes JA, Mestrinho LA, Berg J, et al. Histologic evaluation of mandibular and medial retropharyngeal lymph nodes during staging of oral malignant melanoma and squamous cell carcinoma in dogs. *J Am Vet Med Assoc.* 2019;254(8):938-943. doi:10.2460/javma.254.8.938
16. Beer P, Pozzi A, Bley CR, Bacon N, Pfammatter NS, Venzin C. The role of sentinel lymph node mapping in small animal veterinary medicine: a comparison with current approaches in human medicine. *Vet Comp Oncol.* 2018;16(2):178-187. doi:10.1111/vco.12372
17. Grimes JA, Secrest SA, Wallace ML, Laver T, Schmiedt CW. Use of indirect computed tomography lymphangiography to determine metastatic status of sentinel lymph nodes in dogs with a pre-operative diagnosis of melanoma or mast cell tumour. *Vet Comp Oncol.* 2020; 18(4):818-824. doi:10.1111/vco.12592
18. Callejo FJG, Beltrán DD, Ramos EB, Elena MJM, González MH, Algarra JM. Use of imaging criteria to identify cervical metastases using CT scans in head and neck tumours. *Acta Otorrinolaringol Esp.* 2008;59(6):257-262.
19. Takahashi Y, Takashima S, Hakucho T, et al. Diagnosis of regional node metastases in lung cancer with computer-aided 3D measurement of the volume and CT-attenuation values of Lymph Nodes. *Acad Radiol.* 2013;20(6):740-745. doi:10.1016/j.acra.2013.01.013

20. Grimes JA, Matz BM, Christopherson PW, et al. Agreement between cytology and histopathology for regional lymph node metastasis in dogs with melanocytic neoplasms. *Vet Pathol*. 2017;54(4):579-587. doi:[10.1177/0300985817698209](https://doi.org/10.1177/0300985817698209)
21. Robb R, Hanson D. A software system for interactive and quantitative visualization of multidimensional biomedical images. *Australas Phys Eng Sci Med*. 1991;1(14):9-30.
22. Bland JM, Altman DG. Statistical methods for assessing agreement between two methods of clinical measurement. *Int J Nurs Stud*. 2010;47(8):931-936. doi:[10.1016/j.ijnurstu.2009.10.001](https://doi.org/10.1016/j.ijnurstu.2009.10.001)
23. Nguyen SM, Thamm DH, Vail DM, London CA. Response evaluation criteria for solid tumours in dogs (v1.0): a Veterinary Cooperative Oncology Group (VCOG) consensus document. *Vet Comp Oncol*. 2015;13(3):176-183. doi:[10.1111/vco.12032](https://doi.org/10.1111/vco.12032)
24. Skinner OT, Boston SE, Giglio RF, Whitley EM, Colee JC, Porter EG. Diagnostic accuracy of contrast-enhanced computed tomography for assessment of mandibular and medial retropharyngeal lymph node metastasis in dogs with oral and nasal cancer. *Vet Comp Oncol*. 2018;16(4):562-570. doi:[10.1111/vco.12415](https://doi.org/10.1111/vco.12415)
25. Ng F, Kozarski R, Ganeshan B, Goh V. Assessment of tumor heterogeneity by CT texture analysis: can the largest cross-sectional area be used as an alternative to whole tumor analysis? *Eur J Radiol*. 2013;82(2):342-348. doi:[10.1016/j.ejrad.2012.10.023](https://doi.org/10.1016/j.ejrad.2012.10.023)
26. Soultani C, Patsikas MN, Mayer M, et al. Contrast enhanced computed tomography assessment of superficial inguinal lymph node metastasis in canine mammary gland tumors. *Vet Radiol Ultrasoun*. 2021;62(5):557-567. doi:[10.1111/vru.13002](https://doi.org/10.1111/vru.13002)
27. Milovancev M, Nemanic S, Bobe G. Computed tomographic assessment of sternal lymph node dimensions and attenuation in healthy dogs. *Am J Vet Res*. 2017;78(3):289-294. doi:[10.2460/ajvr.78.3.289](https://doi.org/10.2460/ajvr.78.3.289)
28. Belotta AF, Sukut S, Lowe C, et al. Computed tomography features of presumed normal mandibular and medial retropharyngeal lymph nodes in dogs. *Can J Vet Res Revue Can De Recherche Veterinaire*. 2022;86(1):27-34.
29. Mandrekar JN. Receiver operating characteristic curve in diagnostic test assessment. *J Thorac Oncol*. 2010;5(9):1315-1316. doi:[10.1097/jto.0b013e3181ec173d](https://doi.org/10.1097/jto.0b013e3181ec173d)
30. Smith M. Surgical approach for lymph node staging of oral and maxillo-facial neoplasms in dogs. *J Am Anim Hosp Assoc*. 1995;31(6):514-518. doi:[10.5326/15473317-31-6-514](https://doi.org/10.5326/15473317-31-6-514)
31. Cotter B, Zwicker LA, Waldner C, et al. Inter- and intraobserver agreement for CT measurement of mandibular and medial retropharyngeal lymph nodes is excellent in dogs with histologically confirmed oral melanoma. *Vet Radiol Ultrasoun*. 2022;63(1):73-81. doi:[10.1111/vru.13029](https://doi.org/10.1111/vru.13029)
32. Schöder H, Carlson DL, Kraus DH, et al. 18F-FDG PET/CT for detecting nodal metastases in patients with oral cancer staged N0 by clinical examination and CT/MRI. *J Nucl Medicine Official Publ Soc Nucl Medicine*. 2006;47(5):755-762.
33. Burns GO, Scrivani PV, Thompson MS, Erv HN. Relation between age, body weight, and medial retropharyngeal lymph node size in apparently healthy dogs. *Vet Radiol Ultrasoun*. 2008;49(3):277-281. doi:[10.1111/j.1740-8261.2008.00366.x](https://doi.org/10.1111/j.1740-8261.2008.00366.x)
34. Ku C-K, Kass PH, Christopher MM. Cytologic-histologic concordance in the diagnosis of neoplasia in canine and feline lymph nodes: a retrospective study of 367 cases. *Vet Comp Oncol*. 2017;15(4):1206-1217. doi:[10.1111/vco.12256](https://doi.org/10.1111/vco.12256)
35. Ramos-Vara JA, Beissenherz ME, Miller MA, et al. Retrospective study of 338 canine oral melanomas with clinical, histologic, and immunohistochemical review of 129 cases. *Vet Pathol*. 2000;37(6):597-608. doi:[10.1354/vp.37-6-597](https://doi.org/10.1354/vp.37-6-597)

SUPPORTING INFORMATION

Additional supporting information can be found online in the Supporting Information section at the end of this article.

How to cite this article: Menghini TL, Schwarz T, Dancer S, Gray C, MacGillivray T, Blacklock KLB. Contrast-enhanced CT predictors of lymph nodal metastasis in dogs with oral melanoma. *Vet Radiol Ultrasound*. 2023;1-12. <https://doi.org/10.1111/vru.13254>